Mon. Not. R. Astron. Soc. **000**, 1–?? (2002) Printed 1 February 2008 (MN LATEX style file v2.2)

INTEGRAL observations of the Small Magellanic Cloud

V.A. McBride[1], M.J. Coe[1], A.J. Bird[1], A.J. Dean[1], A.B. Hill[1], K.E. McGowan[1], M.P.E. Schurch[1], A. Udalski[2], I. Soszynski[2], M. Finger[3], C.A. Wilson[3], R.H.D. Corbet[4] and I. Negueruela[5]
[1] *School of Physics and Astronomy, Southampton University, SO17 1BJ, UK*
[2] *Warsaw University Observatory, Aleje Ujazdowskie 4, 00-478 Warsaw, Poland*
[3] *NASA/MSFC, Huntsville, AL 35812, USA*
[4] *USRA, Mail Code 662, NASA/GSFC, Greenbelt, MD 20771, USA*
[5] *Departamento de Fisica, Ingeniera de Sistemas y Teora de la Seal, Escuela Politcnica Superior, University of Alicante, Ap.99, 03080 Alicante, Spain.*

accepted version : 3 Sep 2007

ABSTRACT

The first INTEGRAL observations of the Small Magellanic Cloud (carried out in 2003) are reported in which two sources are clearly detected. The first source, SMC X-1, shows a hard X-ray eclipse and measurements of its pulse period indicate a continuation of the long-term spin-up now covering ∼30 years. The second source is likely to be a high mass X-ray binary, and shows a potential periodicity of 6.8 s in the IBIS lightcurve. An exact X-ray or optical counterpart cannot be designated, but a number of proposed counterparts are discussed. One of these possible counterparts shows a strong coherent optical modulation at ∼ 2.7 d, which, together with the measured hard X-ray pulse period, would lead to this INTEGRAL source being classified as the fourth known high mass Roche lobe overflow system.

Key words: stars:neutron - X-rays: binaries: individual : SMC X-1

1 INTRODUCTION AND BACKGROUND

X-ray satellite observations have revealed that the Small Magellanic Cloud (SMC) contains an unexpectedly large number of High Mass X-ray Binaries (HMXB). At the time of writing, ∼60 known or probable sources of this type have been identified in the SMC and they continue to be discovered at a rate of about 2-3 per year, although only a small fraction of these are active at any one time because of their transient nature. Unusually (compared to the Milky Way and the LMC) all the X-ray binaries so far discovered in the SMC are HMXBs, and equally strangely, only one of the objects is a supergiant system (SMC X-1), all the rest are Be/X-ray binaries. A review of these systems may be found in Haberl & Sasaki (2000) and Coe et al. (2005).

In this paper observations by the INTEGRAL observatory are reported which primarily cover the hard X-ray regime. Since the fully coded field of view of IBIS (Imager on Board INTEGRAL Satellite) extends over 9 degrees, it is possible to view the entire SMC at once. Detailed timing and imaging results are presented.

2 INTEGRAL OBSERVATIONS

The SMC was observed with INTEGRAL during 2003 July and August, corresponding to satellite revolutions 94 and 95, or 155 ks of observing time. Standard processing of the IBIS and JEM-X (Joint European Monitor for X-rays) data was performed using INTEGRAL Off-line Science Analysis (OSA Goldwurm et al 2003) software version 5.1. After basic data correction, good time handling, dead time correction, background correction and event binning, sky images were created for each individual pointing (∼ 2000 s) in the following energy bands: 20–40, 40–60 and 60–100 keV with IBIS and 3–10 and 10–35 keV with JEM-X.

To remove systematic effects in the ISGRI (INTEGRAL Soft Gamma-Ray Imager) detector plane, successive science windows are dithered, resulting in slightly different pointing positions. Thus images incorporating more than one science window need to be mosaicked together. In addition this mosaicking improves the signal and allows one to search for fainter sources which may not appear in a single science window. In the IBIS 20–40 keV mosaic, a section of which is shown in Figure 1, two sources were apparent above the detection limit:

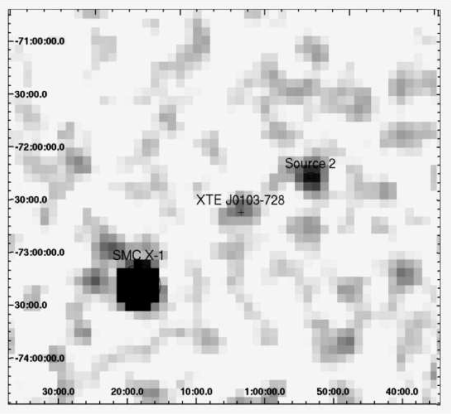

Figure 1. IBIS 20–40 keV image of the SMC. The position of XTE J0103-728 = SXP6.85 is also shown (Haberl et al. 2007).

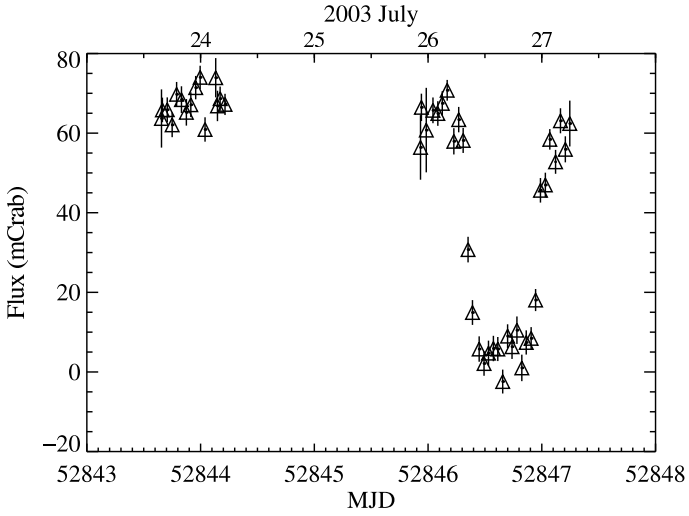

Figure 2. Flux v time in the 20-40 keV band for SMC X-1.

(i) SMC X-1, with a detection significance of 100σ and an average flux of $F_{20-40\,\mathrm{keV}} = 3.2 \times 10^{-10}\,\mathrm{erg\,cm^{-2}\,s^{-1}}$, which corresponds to a luminosity of $1.4 \times 10^{38}\,\mathrm{erg\,s^{-1}}$ at a distance of 60 kpc (Dolphin et al 2001). The source position is determined as $01^{\mathrm{h}}17^{\mathrm{m}}09^{\mathrm{s}}, -73°26'47''$ with a 90% error circle of radius $24''$.

(ii) Source 2, with a detection significance of 9σ and an average flux of $F_{20-40\,\mathrm{keV}} = 2.6 \times 10^{-11}\,\mathrm{erg\,cm^{-2}\,s^{-1}}$, which corresponds to a luminosity of $1.1 \times 10^{37}\,\mathrm{erg\,s^{-1}}$ at a distance of 60 kpc (Dolphin et al 2001). The source position is determined as $00^{\mathrm{h}}54^{\mathrm{m}}10^{\mathrm{s}}, -72°25'44''$ with a 90% error circle of radius $3.4'$.

Although SMC X-1 was apparent in JEM-X observations, Source 2 was not detected with JEM-X.

In Figure 1 we also overplot the position of source XTE J0103-728 (a 6.8s X-ray pulsar), as determined from XMM observations (Haberl et al. 2007). Please note that although this source is not detected in this INTEGRAL observation, the source position is plotted on Figure 1 to aid the discussion in Sect. 5 that Source 2 and XTE J0103−728 are two different sources.

3 TIMING ANALYSIS

3.1 SMC X–1

A lightcurve at science window time resolution (~ 2000 s) was extracted in the 20–40 keV energy range for the epoch MJD 52843 to MJD 52848. Figure 2 clearly shows the source undergoing a hard X-ray eclipse.

SMC X-1 has shown a constant spin-up throughout the history of the source. The spin period of SMC X-1, by far the brightest source in the mosaic, was investigated by extracting time and energy tagged events from the ISGRI detector for 2.95 hours (3 Science Windows) starting at MJD 52843.96. These science windows were chosen as they were consecutive in time and in these observations SMC X-1 was very close (within 3°) to the telescope pointing axis. Events were filtered by selecting only those which have a Pixel Illumination Fraction (PIF) of 1. The PIF is a number, relevant to coded-mask telescopes, between 0 and 1 designating the fraction of a pixel that is illuminated by a source at a given position on the sky. Choosing events based on the criterion that PIF = 1 increases the signal to noise by ensuring that only events from pixels which are totally illuminated by the source contribute. However, photons from other sources in the IBIS field of view may also contribute to events in these pixels as background, and hence, any methods (like this one) which do not involve the construction of a shadowgram are subject to contamination by all other sources in the field. In general, even for an event list selected on the criterion that the PIF for a specific source should equal 1, 95% of the events will be background.

A further filtering, allowing only events at energies between 20 and 100 keV to contribute to the signal, was applied to the event list. The event times were corrected to the Solar System barycentre and corrected to the barycentre of the neutron star-supergiant system, using the orbital ephemeris from Wojdowski et al. (1998).

According to the pulse ephemeris in Naik & Paul (2004), the source is expected to be spinning at a period of 0.7052 s at the start of the observations in our study. An epoch folding technique (Leahy et al., 1983) was used to determine the χ^2 statistic for a number of test periods in the range 0.70 to 0.71 s at a resolution of 0.0001 s. The pulsation period is taken as that with the greatest deviation from a constant flux. Figure 3 shows the χ^2 statistic plotted against period for the SMC X-1 data. The detection of pulsations at 0.704596 ± 0.000008 s is clearly visible. Figure 4 represents the 20–100 keV pulse profile at this pulse period. The pulse profile shows the clear double-peaked structure characteristic of emission from both poles on the neutron star. In addition, the profile in gamma-rays closely resembles that exhibited by SMC X-1 in the hard X-rays (Naik & Paul 2004, Wojdowski et al 1998).

SMC X-1 has shown a constant spin up over the last thirty years of observations. Spin-up is believed to be an effect of accretion torques (Ghosh & Lamb 1979), i.e. matter orbiting in the accretion disc around the neutron star transfers angular momentum to the neutron star when it accretes, spinning up the neutron star. Although some accreting X-ray pulsars show periods of spin-up and spin-down, SMC X-1

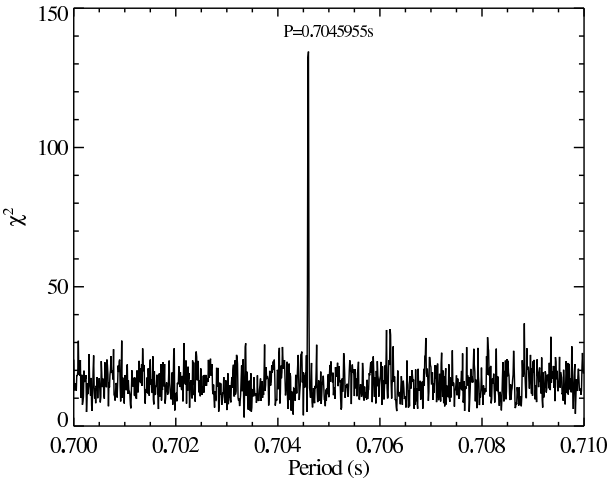

Figure 3. Results of the epoch-folding search for SMC X-1

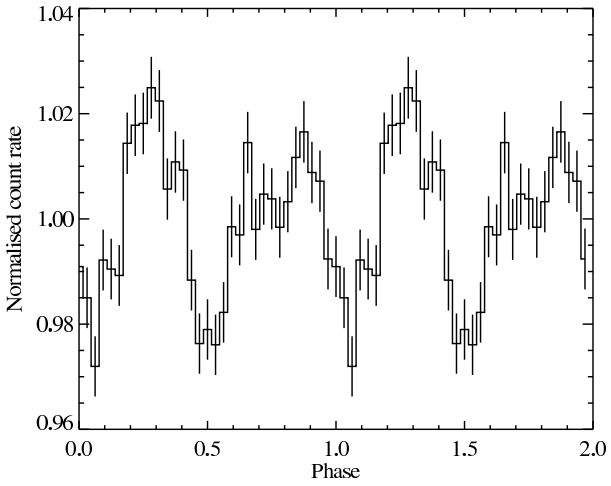

Figure 4. Pulse profile of SMC X–1 in the 20–100 keV band

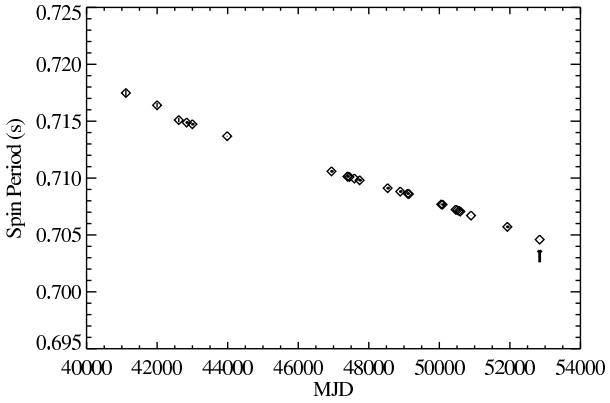

Figure 5. Spin up of SMC X-1 over the last 30 years. The INTEGRAL result is the last in the series and indicated by an arrow.

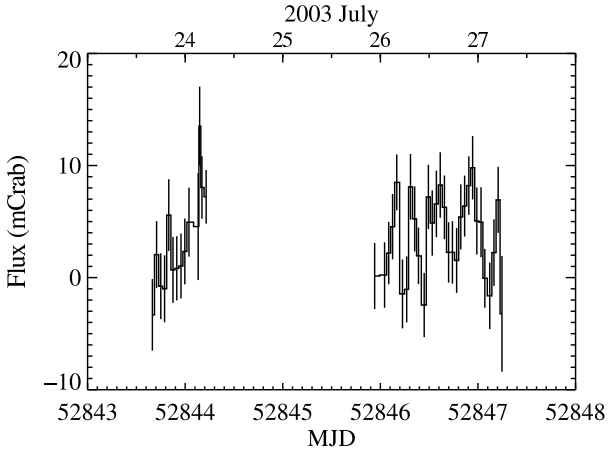

Figure 6. Light curve of Source 2 at Science Window time resolution

is persistently accreting matter from the stellar wind of its supergiant companion hence it has been spinning up for at least as long it has been observed. Figure 5 shows the evolution of the spin period of SMC X-1, with the arrow denoting the measurement made in this work.

3.2 Source 2

Apart from SMC X-1, the INTEGRAL map reveals a second source which we have designated here as Source 2. In the Third IBIS/ISGRI Soft Gamma-ray Survey Catalog (Bird et al, 2007), Source 2 was identified with the nearest ROSAT source: RX J0053.8−7226 at $00^{\rm h}53^{\rm m}53.4^{\rm s}$, $-72^\circ27'01''$. This source (=1WGA J0053.8-7226 =XTE J0053-724), a known Be/X-ray binary in the SMC (Haberl & Pietsch, 2004), has been observed with ROSAT, RXTE and ASCA and has a well-established spin period of 46.6 s (Corbet et al, 1998).

The long term lightcurve of Source 2 is shown in Figure 6 from MJD 52843. During the first block of data (revolution 94) the source appears to be in the process of switching on.

In order to search for the 46.6s spin period of RX J0053.8−7226, we extracted a lightcurve at 1 s time resolution. Instead of creating the source shadowgram, the lightcurves were assembled using the *iilight* tool supplied with OSA 5.1. This tool extracts a lightcurve for every source as well as the background in the field of view by using the Pixel Illumination Function (PIF). The advantage of this method is that lightcurves down to a time resolution 0.1 s can be constructed.

The lightcurve was subjected to a Lomb-Scargle analysis to search for periodicities in the range 2–1000 s (Lomb 1976, Scargle 1982). Although no significant peaks in the periodogram were detected during revolution 94, or the combined lightcurve of revolutions 94 and 95, a marginal periodicity at 6.878 ± 0.001 s was detected in revolution 95 (see Fig. 7). We also searched lightcurves binned at 2, 5 and 20 s, but detected no periodicities above a significance of 90%.

The significance levels overplotted in this Fig. 7 were calculated from 10000 Monte Carlo simulations of the dataset. Each simulated lightcurve had the timestamps of the original lightcurve, but data randomly drawn from a Gaussian distribution around the mean of the original data and with the variance of the original data. A Lomb-Scargle analysis was performed on each lightcurve, and the maxi-

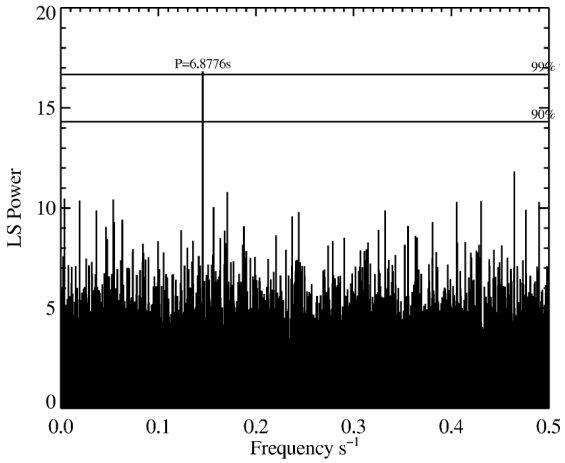

Figure 7. Lomb-Scargle periodogram of Source 2. The solid lines show the 90% and 99% confidence levels determined from the Monte Carlo simulations.

mum power for each of the 10000 lightcurves was noted, and used to generate the cumulative distribution function. From this distribution one can read off the probability of finding a peak of given power in the periodogram due to random noise. The 6.8s peak just exceeds the 99% level (2.6σ).

To explore the significance of both the detection of a 6.8 s period and the non-detection of a 46.6 s periodicity in the data, simulated sine waves of differing periods were added to the existing lightcurve such that the pulse fraction was 100% and then put through the same Lomb-Scargle analysis. These simulations showed that, even at a pulsed fraction of 100%, a 46.6 s periodicity would be unlikely to show up above the noise. For this same reason we note that the detection of the 6.8 s periodicity is only at the 99% significance level and may be spurious.

The non-detection of a 46.6s periodicity in the lightcurve from Source 2 means that the identity of this source still remains an open question. Although it may yet be shown that Source 2 can be identified with RX J0053.8−7226, it is also a likely possibility that Source 2 may be another X-ray binary in the SMC with a pulse period ~ 6.8 s. We explore these options further in Sect. 5.

4 SPECTRAL MODELLING

4.1 SMC X–1

A source spectrum in the energy range 3–100 keV is shown in Figure 8, using data from the JEM-X (3–25 keV) and IBIS (20–100 keV) detectors. This spectrum combines all spectra from individual observations of SMC X-1 during revolutions 94 and 95. The JEM-X spectrum is generated by combining spectra from individual science windows during which the source was within 7.5° of the pointing axis. During all these observations SMC X-1 was in the high state of its 40–60 d super-orbital cycle (Clarkson et al., 2003), so spectral parameters will vary from observations taken during the low state. Spectral fitting was performed using XSPEC v11.3.1 (Arnaud 1996).

We fitted thermal bremsstrahlung and power law models to the data. Because the data do not cover energies below 3 keV, in both cases we constrained the absorption column between a lower limit of 4.64×10^{20}atoms cm^{-2}, the estimated neutral hydrogen density in a cone of radius 1° in the direction of the SMC (Dickey & Lockman 1990) and an upper limit of 9×10^{21} atoms cm^{-2}, the highest value of $N_{\rm H}$ recorded by Woo et al., (1995). The best fit ($\chi^2_\nu = 1.14$) was achieved using a photoelectric absorption component, with cross-sections from Balucinska-Church & McCammon (1992) and abundances from Anders & Grevesse (1989), with a high energy cutoff power law model. No emission from FeKα, which is often seen in X-ray binaries and has been noted in SMC X-1 on a previous occasion (Naik & Paul 2004), was detected. The spectral parameters for the best fit model are given in Table 1.

Table 1. Spectral parameters for an exponentially cutoff power law model fit to SMC X-1.

	Our work		Naik & Paul (2004)
Param	Value	Param	Value
$N_{\rm H}$	$3.8^{+5.1}_{-3.3} \times 10^{21}$cm^{-2}	$N_{\rm H}$	$2.55 \pm 0.09 \times 10^{21}$cm^{-2}
Γ	0.57 ± 0.07	Γ	0.82 ± 0.02
$E_{\rm cut}$	4.3 ± 0.5 keV	$E_{\rm cut}$	6.3 ± 0.09 keV
$E_{\rm fold}$	$9.2^{+0.1}_{-0.2}$ keV	$E_{\rm fold}$	10.58 ± 0.13 keV
		kT	0.19 ± 0.01 keV
χ^2(dof)	168(145)	χ^2_ν(dof)	1.3(168)

Comparing the ISGRI spectrum to previous studies of the broadband spectrum of SMC X-1 will allow us to notice whether there are any long term spectral changes in the source. Prior to these data, the most recent broadband (0.1–80 keV) spectral analysis of SMC X-1 was undertaken by Naik & Paul (2004) using data obtained between 1997 January to April from the three detectors on board *BeppoSAX*. A best fit was obtained by modelling the data with a power law with a high energy cutoff, a thermal blackbody component to account for emission in the soft part of the spectrum, and a weak Fe line.

The data from the current observation extend down to 3 keV, i.e. not low enough in energy to allow us to investigate the soft blackbody component that makes its major contribution below energies of 1.0 keV. Similarly, the column density for our observations is not well constrained without data below 3 keV. Although the parameters for the power law slope (Γ), and the $E_{\rm cut}$ differ substantially from those obtained by Naik & Paul (2004), if we fix the $E_{\rm cut}$ at 6.3 keV we can recover, within errors, the same power law slope as measured in their observations. Thus, in general, our continuum models agree with those of Naik & Paul (2004) and hence we note that no significant changes in the continuum X- and γ-ray emission took place between these two observations.

Naik & Paul (2004), however, report the detection of a weak FeKα emission line, which we find no evidence for in this observation. Fe emission is also reported by Woo et al. (1995) in a *Ginga* observation from 1989. We attribute the non-detection of an Fe emission component to the lower sensitivity of the JEM-X instrument. The Fe line flux as reported by Naik & Paul (2004) is 1.4×10^{12} erg cm^{-2} s^{-1}, which converts into 1.5×10^{-4} photons cm^{-2} s^{-1} at 6.4 keV.

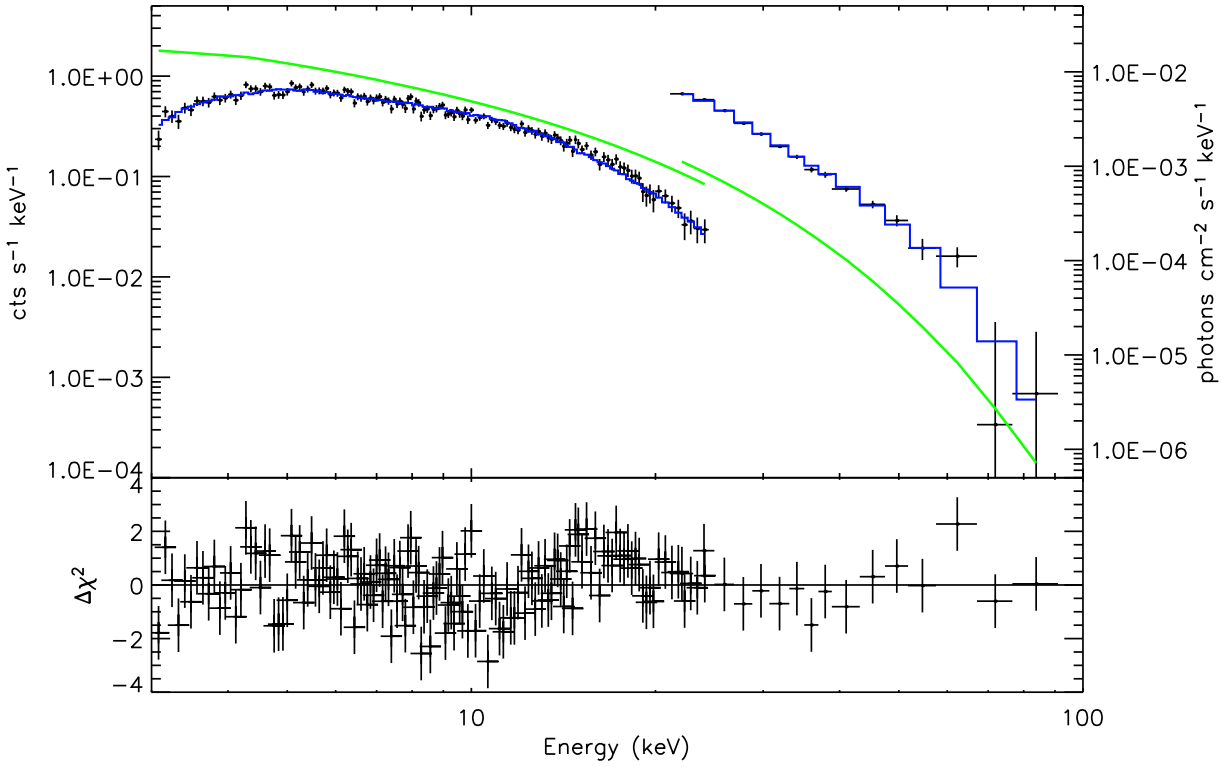

Figure 8. 3-100 keV spectrum of SMC X-1 fitted with a Comptonisation model. The black crosses show the data points, the histogram the fitted model, and the grey line shows the unfolded model and is plotted on the secondary Y-axis.

This is below the JEM-X line sensitivity, which is 1.6×10^{-4} photons cm^{-2} s^{-1} at 6 keV. We note that the lack of the Fe emission line at ~ 6.4 keV in our dataset may contribute to shifting the $E_{\rm cut}$ to softer energies.

Kunz et al. (1993) examine the X-ray spectral properties of SMC X-1 in the 20–80 keV energy band during observations by *HEXE* between 1987 November and 1989 March. They describe the continuum by fitting a thin thermal bremsstrahlung model. Although our data are not fit at all well by the above model, if we restrict our energy range to 20–80 keV, using only the IBIS spectrum, a thermal bremsstrahlung model gives an adequate fit and plasma temperature of 12.2 ± 0.4 keV; close to the plasma temperature of 14.4 ± 0.13 keV by Kunz et al. (1993). We can conclude that taking the low energy data into account rules out the thermal bremsstrahlung model.

4.2 Source 2

The ISGRI spectrum of Source 2 from 20–100 keV was best fit with a power law of slope 2.6 (χ^2(dof)=7.2(3)). Other models, such as a power law with a high energy exponential cutoff, Comptonisation, and thermal bremsstrahlung models were used with less successful results.

Although a soft power law is the best model to describe the data in the IBIS energy range, it may not be appropriate across the entire energy range. Measures of the absorption column and blackbody contributions to the spectrum often come into play at energies between 0.1 and 3 keV. The source is not detected in ~ 149 ks of simultaneous JEM-X observations. Using the power law parameters derived from the fit to the IBIS data we estimate the flux in the JEM-X 5–10 keV range to be $\sim 6 \times 10^{-11}$ erg cm^{-2} s^{-1}. With a very bright source (SMC X-1) in the field of view it is clear that Source 2 is at or below the JEM-X detection limit.

5 DISCUSSION

In this section we discuss the possible counterparts for Source 2.

A pulsar, XTE J0103−728 = SXP6.85, with spin period 6.8482 ± 0.0007 s has previously been reported in the SMC (Corbet et al., 2003). On the basis of the similarity of their periods it is tempting to assume that this object is the same as the INTEGRAL Source 2. However, recent XMM-Newton observations (Haberl et al. 2007) have located this pulsar to within 2″ at a position some 40′ away from the INTEGRAL source (see Fig. 1). Furthermore, Galache et al. (2007) report, in their RXTE monitoring of pulsars in the SMC, that SXP6.85 was not detected around the time of the INTEGRAL observations. The nearest RXTE measurement (about 30–40 d later) confirms that the periods are close, but distinctly different. Based on the clear discrepancies in both the positions and the pulse periods, we conclude that XTE J0103−728 can not be the counterpart to Source 2.

Chandra X-ray observations of the region around Source 2 during 2002 July and 2006 April detect 11 X-ray sources within the INTEGRAL error circle, of which three correlate with previously known objects in the Simbad database and have V$\sim$ 15 optical counterparts. These

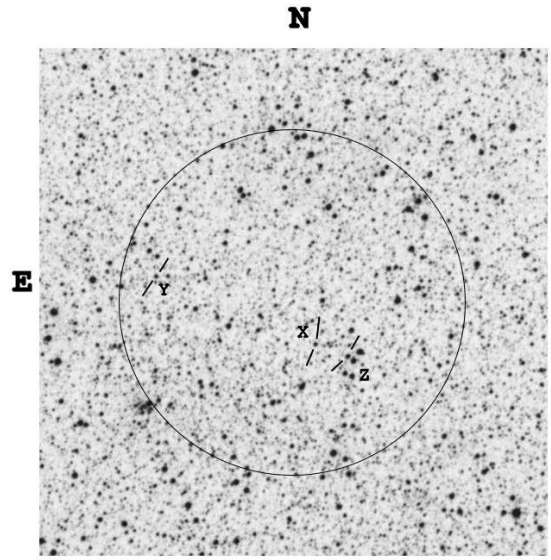

Figure 9. Finding chart showing the position of the INTEGRAL 90% uncertainty circle for Source 2. The circle has a radius of 3.4 arcmin. Indicated as X, Y & Z are the three bright (V∼15) optical objects that coincide with Chandra X-ray sources.

objects are labelled X, Y and Z in Figure 9 and have the following identifications:

(i) Object X at $00^{\rm h}54^{\rm m}03.7^{\rm s}, -72^\circ26'33.1''$ is SMC 28942 from Massey (2002) with $V = 14.81$, $B - V = -0.04$
(ii) Object Y at $00^{\rm h}54^{\rm m}46.2^{\rm s}, -72^\circ25'23.0''$ is SMC 31155 from Massey (2002) and identified as object 798 in the catalogue of Meyssonnier & Azzopardi (1993) with $V = 15.25$, $B - V = -0.10$.
(iii) Object Z at $00^{\rm h}53^{\rm m}55.2^{\rm s}, -72^\circ26'45.7''$ is SMC 28479 from Massey (2002) with $V = 13.98$, $B - V = -0.09$.

All sources were too faint in the Chandra X-ray data to perform a timing analysis, which would have been the most direct means of linking any of them with Source 2.

Long-term OGLE optical photometric data in the I band were examined for all three objects. Objects X & Z exhibit significant variability patterns of 0.3–0.5 mag over several years, characteristic of the behaviour of Be stars (Mennickent et al., 2002). However, subjecting the data to a frequency search using a Lomb-Scargle routine reveals nothing periodic in the search range of 1.5 – 200 days. The third object (Y), however, shows much smaller changes of the order of 0.05 mags over many years (see Figure 10). More importantly, the Lomb-Scargle search reveals a strong and clear modulation at a period of 2.71443±0.00012 d. Also evident in Figure 10, which shows the results from searching the period range 1.5–5 d, is the beat period of the 2.71 d with the 1 d sampling.

Chandra source Z has been firmly associated with the Be/X-ray binary system RX J0053.8−7226 =1WGA J0053.8−7226 =SXP46.6 (Coe et al. 2007), which has a pulse period of 46.6 s. As can be seen from Fig 9, the source position is consistent with the IBIS position of Source 2. Futhermore, RXTE has observed RX J0053.8−7226 in outburst during a Type I periastron passage at the time of the INTEGRAL observation (Galache et al. 2007). Extrapolation of the X-ray flux from RX J0053.8−7226 observed during this outburst into the IBIS 20–40 keV energy range (estimating a pulsed fraction of 0.2 and a photon index of 1) shows that RX J0053.8−7226 should be detected at the 11σ level with IBIS – i.e. consistent with the current level at which Source 2 has been detected.

As the spatial and flux information, as well as the epoch of observation of Source 2, are all compatible with reasonable assumptions about the behaviour of RX J0053.8−7226, the simplest conclusion is that Source 2 as observed by IBIS can be identified with RX J0053.8−7226 as initially suggested by Bird et al (2007). However, this conclusion is by no means secure, as equally reasonable extrapolations of the RXTE flux from RX J0053.8−7226 (using a pulsed fraction of 0.5 and a photon index of 2) yield a source that would be well below the detection limit of IBIS. In addition to this, it is nescessary to account for the lack of detection of a 46.6 s periodicity, and instead the possible detection of a 6.8 s periodicity in the data from Source 2.

The simplest explanation is that a low pulse fraction, combined with the low flux source detected by IBIS, makes the 46.6 pulsations undetectable. This does not, however, explain the presence of the 6.8 s pulsations detected in the IBIS data. If this detection is real then RX J0053.8−7226 cannot be the counterpart to INTEGRAL Source 2. The simulations we have performed in Sect. 3.2 indicate that the detection of pulsations is marginal at this flux/exposure, and requires an extremely high pulsed fraction for this particular dataset. While the power of the 6.8 s pulsations is strong, we cannot rule out the possibility that the detection is spurious.

With these concerns raised, we also consider possible scenarios in the case that RX J0053.8−7226 (Chandra source Z) is not the counterpart to Source 2.

We have little information on Chandra source X except that its optical properties resemble those of source Z. We could consider this a point in favour of X being the counterpart to IBIS Source 2, which may then indicate that Source 2 is likely to be a Be/X-ray binary.

If Chandra source Y, with its 2.7 d optical periodicity were the counterpart to Source 2 (with its 6.8 s pulse period), this object would occupy a unique corner of the Corbet diagram (see Fig. 11), indicating that the source may be a Roche Lobe Overflow (RLOF) system. Thus far only three RLOF systems are known: SMC X-1, Cen X-3 and LMC X-4 and adding another object to this class of sources would be an exciting prospect. To investigate this possibility we examine some of the X-ray and optical properties of Chandra source Z and IBIS Source 2 and compare them with those of the known RLOF systems.

A search through the Chandra archives reveals three observations of this region on 2002 July 20, 2006 April 25 and 26. Chandra source Y was detected on all three occasions and exhibits a flux varying by a factor of ~ 10. Existing RLOF systems display persistent emission which varies between high and low states at superorbital periods. If Source 2 and Chandra source Y are indeed the same source, they have

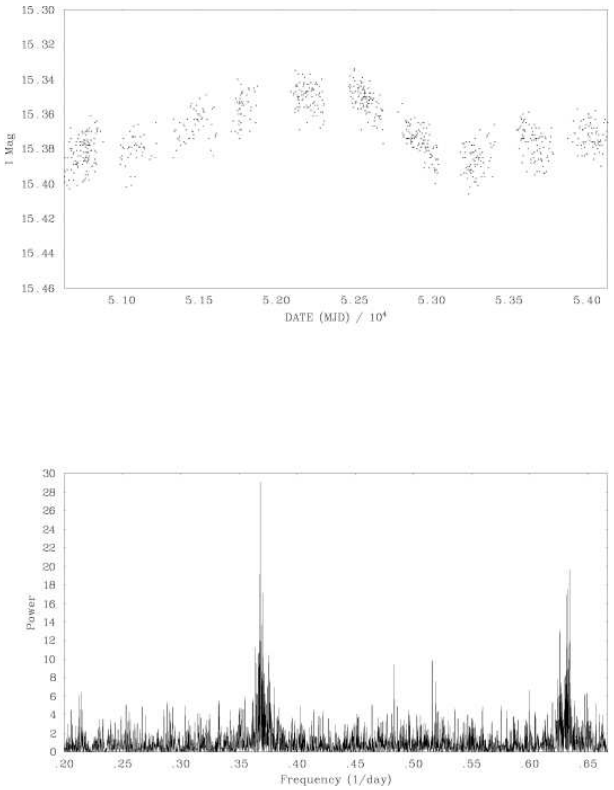

Figure 10. Top: the OGLE I-band light curve over 10 years for Object Y. Lower: the associated Lomb-Scargle power spectrum of Object Y showing a peak at a period of ∼2.7 d.

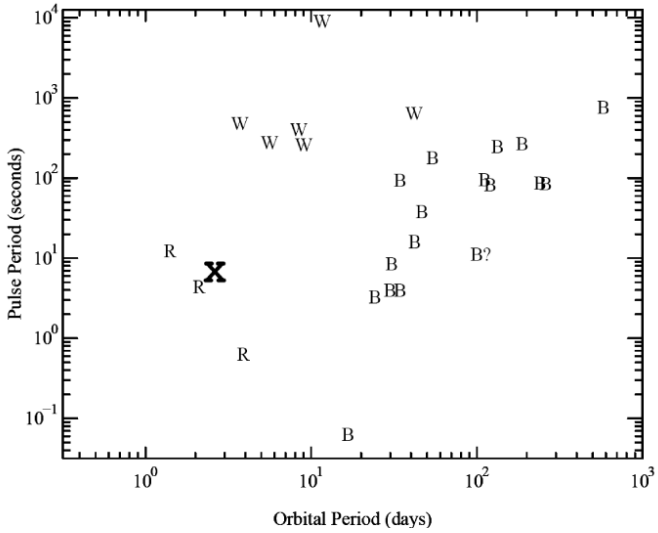

Figure 11. The Corbet diagram (modified from Corbet et al. 1999) showing the location of INTEGRAL Source 2 marked with the X symbol (see text for assumptions made in locating the source at this position). The B symbol indicates a Be star system, the W indicates a wind-fed system and the R symbol indicates the Roche-lobe overflow systems.

been observed, at varying flux levels, in all four observations of this region.

The optical magnitudes and colours of source Y are consistent with those of an early-type, luminosity class III-V star, similar to the optical counterpart of LMC X-4 (Hutchings, Crampton & Cowley 1978). Furthermore, when X-ray colours are used to locate this object on the colour-colour diagram for SMC sources (McGowan et al, 2007), source Y sits comfortably in the middle of the known pulsar systems.

6 CONCLUSIONS

This work has shown that SMC X-1 continues its secular spin-up trend, with the latest pulse period measurement being 0.704596 ± 0.000008 s. We can also conclude that the broadband spectrum of SMC X-1 is roughly consistent from 1987 through 2004.

We have discovered a potential 6.8 s periodicity in the IBIS data from Source 2, which casts some doubt on its current identification as the counterpart to RXJ 0053.8-7226. We conclude on the basis of spatial and timing information that Source 2 is not related to XTE J0103−728 – a previously known Be/X-ray binary with a pulse period of 6.85 s. Archival Chandra observations are used to investigate the feasibility of other X-ray/optical counterparts to the sources. We can conclude from this work that it is highly probable that Source 2 is a HMXB and, depending on its X-ray/optical associations, may yet turn out to be one of a small number of Roche Lobe Overflow HMXB systems. If this were the case, it is intriguing both why Source 2 has not been detected with previous X-ray missions (could it be obscured somehow in the softer X-rays?) and also, why three out of the four known RLOF systems have evolved in the Magellanic Clouds.

To resolve this situation, detection of either the 46.6 s period in IBIS Source 2, or the 6.8 s period in either of the Chandra sources X or Y would be required and further observations are encouraged.

7 ACKNOWLEDGEMENTS

VAM acknowledges support from the South African NRF and the British Council in the form of a SALT/Stobie studentship.

REFERENCES

Anders E. & Grevesse N. 1989, Geochim. Cosmochim. Acta, 53, 197

Arnaud K. A. 1996,ASP Conf. Ser. 101: Astronomical Data Analysis Software and Systems V, eds. Jacoby G.H. and Barnes J.

Balucinska-Church M. & McCammon D. 1992, ApJ, 400, 699

Bird A. J. et al., 2007, ApJS 170, 175.

Clarkson W.I., Charles P.A., Coe M.J., Laycock S., Tout M.D. and Wilson C.A., 2003 MNRAS 339, 447.

Coe, M. J., Edge, W. R. T., Galache, J. L. & McBride, V. A. 2005 MNRAS 356, 502.

Coe, M.J., McGowan, K.E. and Schurch, M.P.E., 2007, in preparation.

Corbet, R. H. D.; Marshall, F. E.; Peele, A. G.; Takeshima, T. 1999 ApJ 517, 956.
Corbet R., Marshall F. E., Lochner J. C., Ozaki M., Ueda Y., 1998, IAU Circular, 6803, 1
Corbet R. H. D., Markwardt C. B., Marshall F. E., Coe M. J., Edge W. R. T., Laycock S., 2003, The Astronomer's Telegram, 163, 1
Dickey J. M., Lockman F. J., 1990, ARA&A, 28, 215.
Dolphin, A. E., Walker, A. R., Hodge, P. W., Mateo, M., Olszewski, E. W.. Schommer, R. A., Suntzeff, N. B. 2001 ApJ 562, 303.
Galache J.L., Corbet R.H.D., Coe M.J., Schurch M. & Laycock S.G.T. 2007, ApJ (submitted).
Ghosh P., Lamb F. K., 1979, ApJ, 234, 296
Goldwurm, A., David, P. and Foschini, L. et al. 2003, A&A 411, 223
Haberl F. & Sasaki M., 2000, A&A 359, 573.
Haberl F., Pietsch W., 2004, A&A, 414, 667
Haberl F., Pietsch W. & Kahabka P., 2007, ATEL 1095.
Hutchings J.B., Crampton D. & Cowley A.P., 2007, ApJ 225,548
Kunz M., Gruber D. E., Kendziorra E., Kretschmar P., Maisack M., Mony B., Staubert R., Dobereiner S., Englhauser J., Pietsch W., Reppin C., Trumper J., Efremov V., Kaniovsky S., Kusnetzov A., Sunyaev R., 1993, A&A, 268, 116
Leahy D. A., Darbro W., Elsner R. F., Weisskopf M. C., Kahn S., Sutherland P. G., Grindlay J. E., 1983, ApJ, 266, 160
Lomb N. R., 1976, Ap&SS, 39, 447
Massey P., 2002 ApJS 141, 81
McGowan K.E. et al., 2007 MNRAS 376, 759.
Mennickent R.E., Pietrzynski G., Gieren W. & Szewczyk O., 2002 A&A, 393, 887.
Meyssonnier N. & Azzopardi M., 1993 A&AS 102, 451
Naik S., Paul B., 2004, A&A, 418, 655
Scargle J. D., 1982, ApJ, 263, 835
Wojdowski P., Clark G. W., Levine A. M., Woo J. W., Zhang S. N., 1998, ApJ, 502, 253
Woo J. W., Clark G. W., Blondin J. M., Kallman T. R., Nagase F., 1995, ApJ, 445, 896